Mon. Not. R. Astron. Soc. 000, 1–14 (2001) Printed 23 December 2002 (MN LaTeX style file v1.4)

Intermediate-metallicity, high-velocity stars and Galactic chemical evolution

S. G. Ryan & I. M. Smith
Dept of Physics & Astronomy, The Open University, Walton Hall, Milton Keynes, MK7 6AA, UK.
s.g.ryan@open.ac.uk; ims83@open.ac.uk

ABSTRACT

High-S/N spectra were obtained of 10 high-proper-motion stars having $-1\lesssim$ [Fe/H] $<$ 0, and a comparable number of disc stars. All but two of the high-proper-motion stars were confirmed to have [Fe/H] > -1.0, some approaching solar metallicity, but even so, earlier measurements overestimated the metallicities and velocities of some of these stars. Models of stellar Populations were used to assign membership probabilities to the Galactic components to which the high-velocity stars might belong. Many were found to be more probably thick-disc than halo objects, despite their large space motions, and two might be associated with the inner Galaxy. It may be necessary to reassess contamination of previous halo samples, such as used to define the metallicity distribution, to account for contamination by high-velocity thick-disc stars, and to consider possible subcomponents of the halo.

The change in [α/Fe] ratios at [Fe/H] $\simeq -1.0$ is often used to constrain the degree and timing of SN Ia nucleosynthesis in Galactic chemical-evolution models. [Ti/Fe] values were measured for eight of the high-velocity stars. Both high- and low-[Ti/Fe] halo stars exist; likewise high- and low-[Ti/Fe] thick-disc stars exist. We conclude that the [Ti/Fe] "break" is not well defined for a given population; nor is there a simple, continuous evolutionary sequence through the break. Implications for the interpretation of the [α/Fe] break in terms of SN Ia timescales and progenitors are discussed. The range of [Ti/Fe] found for *high*-velocity (low rotation) thick-disc stars contrasts that for the *low*-velocity (high rotation) thick-disc sample studied by Prochaska et al.

Key words: stars: abundances – stars: Population II – Galaxy: halo – Galaxy: kinematics and dynamics – Galaxy: structure – nuclear reactions, nucleosynthesis, abundances

1 INTRODUCTION

1.1 Stellar Populations

A simple picture of the stellar populations in the Galaxy might describe two main components: The dominant Population I disc has scale heights from a few hundred parsecs for thin-disc stars up to one thousand parsecs for thick-disc stars, metallicities extending down to about one tenth solar, and ages younger than 6-10 Gyr (from measurements of NGC 188 (6 Gyr; Dinescu et al. 1995), NGC 6791 (8 Gyr; Chaboyer, Green & Liebert 1999), and white dwarfs in the disc (10 Gyr; Oswalt et al. 1996)). The scarce, Population II halo stars may travel many kpc from the disc, are older than 10 Gyr, and have a mean metallicity one fortieth solar.

In reality, the division of populations is not so straightforward as described above, and there exist stars having characteristics of both groups. Examples include overlapping thick and thin disc populations (Wyse & Gilmore 1995), *in situ* halo samples such as RR Lyraes (Saha 1985), and the globular cluster Terzan 7, associated with the Sagittarius dwarf (Da Costa & Armandroff 1995; [Fe/H] ~ -0.4), all of which have metallicities exceeding one tenth solar. A contrasting group are stars with rapid rotation about the Galaxy but metallicities below one tenth solar (Beers et al. 2002), the metal-weak thick-disc stars, which overlap in metallicity with the halo.

This paper is concerned with another non-conforming group: high-velocity dwarfs with kinematics resembling those of halo stars, but having metallicities exceeding one tenth solar. Such stars can be identified in the proper-motion-selected samples studied by Laird, Carney & Latham (1988a) and Ryan & Norris (1991a,b). The present study was undertaken to characterise these stars better, seek clues to their origin, and assess their implications for our understanding of Galactic chemical evolution.

High-velocity, metal-rich stars could belong to one of a

© 2001 RAS

number of possible subgroups in the Galaxy. The most obvious is the standard halo population, in which case they would represent the metal-rich tail of the Pop. II metallicity distribution. They might be kinematically-extreme members of the thick disc, or alternatively they could be lower-mass counterparts of the young, high-velocity A-stars identified by Rodgers, Harding & Sadler (1981) and Stetson (1981a). The A-stars appear to be almost coeval at an age < 0.65 Gyr, and do not appear to fit into the usual Galactic populations (Lance 1988). Such objects were proposed by Rodgers et al. to have formed in a recent merger of a Magellanic Cloud-like, gas rich satellite with the Galaxy. The vertical velocity dispersion of the A-stars, $\simeq$60 km s^{-1}, is sufficiently low that it would be difficult to distinguish their lower-mass counterparts from other normal halo or thick disc stars on the basis of kinematics and composition alone. There are some dwarfs, however, which lie blueward of the Population II main sequence turnoff, and therefore appear younger than the bulk of the halo. Such stars could be field blue stragglers, but they could also be counterparts of the Rodgers et al. A-stars.

Faced with various non-conforming stars, it is important to recall the difficulty of disentangling merged populations. For example, Preston, Beers & Shectman (1994) argued initially that most of the blue metal-poor (BMP) stars they observed had younger ages than halo and thick-disc stars, and kinematics intermediate to those components. They suggested that these stars originated in a dwarf satellite galaxy that was accreted by the Milky Way. However, a subsequent, extended analysis (Preston & Sneden 2000) suggested instead that a large fraction (60 – 100%) were blue stragglers after all, and hence presumably of Galactic origin.

1.2 Galactic chemical evolution

Non-conforming stars can challenge and inform our understanding of the chemical evolution of the Galaxy. Halo stars with [Fe/H] $<$ -1.0 have fairly uniform overabundances of [Ti/Fe] in the range 0.3 to 0.5, whereas in disc stars [Ti/Fe] evolves from $\sim$0.3 at [Fe/H] = -1.0, to 0.0-0.1 at [Fe/H] = 0.0 (*e.g.* Edvardsson et al. 1993; Chen et al. 2000). The apparent change in the trends of [α-element/Fe] (e.g. [O/Fe]) versus [Fe/H] at [Fe/H] $\simeq$ -1.0 is regarded as an important constraint in Galactic chemical evolution models, but its interpretation may not be as simple as is often stated. The usual explanation, following Tinsley (1979), is that stars with [Fe/H] $<$ -1.0 formed from material enriched primarily by SN II's, which are relatively poor producers of iron, while more metal-rich stars formed after the appearance of SN Ia's, whose element yields are more iron rich than SN II's. Because of the much shorter lifetimes of SN II progenitors (high-mass stars of $M \gtrsim 8$ M$_\odot$) compared to the progenitors of SN Ia's, the break in [α/Fe] is conventionally taken to signify the appearance of SN Ia's only after enrichment of the Galaxy to [Fe/H] $\simeq -1.0$, and thus the evolutionary timescales of the SN Ia progenitors provide valuable constraints on the metal enrichment of the Galaxy.

The *mechanism* for SN Ia's is believed to be the attainment of the Chandrasekhar mass by a white dwarf. However, the *progenitors* of SN Ia's are not known with certainty, and possibilities include the merger of two white dwarfs in double-degenerate systems, and the accretion of mass onto a white dwarf from a non-degenerate companion in the single-degenerate scenario. The former mechanism proceeds on a slow orbital decay time-scale, the first events occurring after 10^8 yr, but having a long tail extending out to 10^{10} yr (Tutukov & Yungelson 1994; Smecker-Hane & Wyse 1992), rather than on the shorter evolutionary time-scale (10^6-10^7 yr) of SN II progenitors. The single-degenerate mechanism depends on the evolutionary timescales of the mass donors, which must be in binaries close enough to undergo mass transfer, beginning after 0.6 Gyr (Kobayashi et al. 1998) .

In the standard framework, the inferred appearance of SN Ia products at [Fe/H] = -1.0 has been used to deduce that the formation of halo stars was completed before SN Ia appeared, in less than 1 Gyr. However, caveats within, and complete departures from, this framework are possible; these possibilities must also be considered in interpreting the observations. Issues include:

Distinguishing evolutionary time from absolute time in a fragmented halo: The [α/Fe] break, if it measures time at all (see below), depends on the time that elapses from the formation of the first SN Ia progenitors in an evolutionary system (e.g. Wyse & Gilmore 1988). As noted by Smecker-Hane & Wyse (1992), efforts to infer timescales from the [α/Fe] break assume a smooth evolutionary sequence from halo, through thick disc, to thin disc. However, it has been suggested that the halo assembled from many independently evolving fragments (e.g. Searle & Zinn 1978). Evidence that at least some fraction of the halo is populated by the debris of such objects comes from the discovery of the Sagittarius dwarf (Ibata, Gilmore & Irwin 1995) and star streams (Helmi et al. 1999).

Independently-evolving fragments need not have begun forming stars simultaneously, so could possess a range of ages and hence not be part of a smooth evolutionary sequence (e.g. Carney, Latham & Laird 1990b; Carney 1996). Globular clusters and Local Group dwarf galaxies provide some guidance on possible age spreads in the Galactic halo. Saviane, Rosenberg & Piotto (1999) and VandenBerg (2000) differ on whether clusters with [Fe/H] < -1 are coeval, but agree that there is no age spread exceeding 2 Gyr at *fixed* [Fe/H] in this interval. In contrast, at higher metallicity there is clear evidence on an age spread of a few Gyr, based on young clusters like Terzan 7, a member of the Sagittarius dwarf which is merging with the Milky Way. (An age spread of a few Gyr was found for metal-poor halo field stars by Schuster & Nissen (1989), though greater potential errors challenge the field-star analysis.) The lack of an age spread amongst halo globular clusters *at fixed metallicity* contrasts with the varied star-formation histories of the dwarf galaxies where a range of star formation histories, and hence stellar ages, are seen (Mateo 1998; Hernandez, Gilmore & Valls-Gabaud 2000). The differences between globular clusters and dwarf galaxies may be important in determining the appearance of the halo field today; abundances anomalies in globular clusters that are not shared by field halo stars may indicate that the latter descended from lower-density systems more like dwarf galaxies.

Independently-evolving fragments which began forming stars at different times would produce SN Ia's, and [α/Fe] breaks, at different times. However, the [Fe/H] scale against which [α/Fe] values are normally plotted is not an absolute time axis. Fragments experiencing the same star formation rate would be expected to reach the same [Fe/H] after the same time has elapsed since the formation of the SN Ia progenitors, irrespective of the absolute time at which star formation begins. In this case they would exhibit the same [α/Fe] vs [Fe/H] behaviour despite differences of potentially several Gyr in the absolute times at which this event occurs. That is, age differences between independently-evolving fragments are not sufficient to produce observable differences in the element abundance trends (e.g. Carney et al. 1990b). If the *star formation rate* varies from one fragment to another, as in the Local Group dwarf galaxies, then different metallicities would be reached by the time the first SN Ia appeared, and in this case each fragment would show its break at a different [Fe/H] (Wheeler, Sneden & Truran 1989; Gilmore & Wyse 1991.) This has been proposed as the explanation of the low-[α/Fe] stars at [Fe/H] $<$ -1 (Peterson 1981; Carney & Latham 1985; Carney et al. 1997; King 1997).

Smecker-Hane & Wyse (1992) noted that the absence of a large spread in element abundances around the break implies that halo fragments, if they existed, must have completed their evolution prior to [Fe/H] = -1 being reached, and prior to the appearance of SN Ia's. They concluded that independent fragments could not be responsible for halo stars observed around the break, and therefore that the formation epoch for stars at the break is not related simply to the time lag for the appearance of SN Ia's.

Distinguishing one evolutionary sequence from a superposition of two: Timing arguments for the [α/Fe] break presume that stars with [Fe/H] < -1 and those with [Fe/H] $>$ -1 lie on a continuous evolutionary sequence. However, observations are dominated by halo stars at [Fe/H] < -1 and by disc stars at [Fe/H] > -1. It has yet to be established whether there is an evolutionary flow from the halo population to the disc, or what [α/Fe] does at this transition. In this view, a plot of [α/Fe] vs [Fe/H] around [Fe/H] = -1 would represent a superposition of two populations on one diagram, and the break would have no evolutionary significance other than indicating the metallicity at which the halo metallicity distribution becomes poorly populated and the disc metallicity distribution began to be significantly populated.

Nissen & Schuster (1997) selected a number of halo stars at [Fe/H] > -1, and found [α/Fe] to range fully from the disc value to the halo value. Their low [α/Fe] ratios were sometimes, but not uniquely, associated with the most extreme kinematics (see also Carney 1999). It therefore appears unsafe to speak of a break for halo stars, since at [Fe/H] > -1 halo stars with both high and low [α/Fe] values exist.

The fact that the apparent break in stellar element ratios *and* changes in stellar kinematics both occur at the same [Fe/H] was discussed extensively by Wyse & Gilmore (1988). However, this likewise could result from a superposition of two distinct populations, disc and halo dominating the view above and below [Fe/H] $\simeq$ -1.0, rather than due to a *change* in chemical and dynamical evolution as part of a continuous evolutionary sequence.

Although we do not claim that globular clusters and field stars have identical evolutionary histories, it is nevertheless appropriate to note the result of Carney's (1996) examination of a sample of globular clusters that span the metallicity of the purported break in field stars. In that work, three clusters with $-0.8 <$ [Fe/H] < -0.5 and thirteen with [Fe/H] < -1.0 show $\langle$[α/Fe]$\rangle$ to be constant irrespective of [Fe/H]. That is, no break is seen for these objects. It is possible that the environments associated with the formation of globular clusters that survive to this day were significantly different to those in which the current field stars are observed, but the lack of a break for globular clusters reinforces the view that a break need not occur in all stellar systems.

Distinguishing metallicity-dependent processes: Kobayashi et al. (1998) have suggested that single-degenerate SN Ia are suppressed at [Fe/H] < -1 due to the formation of a common-envelope system when the metallicity (opacity) of the gas is low. It is therefore possible that the break in [α/Fe] provides no timing information, and instead is solely a reflection of the appearance of single-degenerate SN Ia once a star-forming environment reaches [Fe/H] = -1, irrespective of how long it took to reach that situation.

Questioning the role of SN Ia: An even more iconoclastic possibility was raised by Chieffi et al. (2002) who noted (their Figure 5) that the [α/Fe] yields of SN II may be so sensitive to progenitor mass that changes in the masses contributing to Galactic enrichment, such as lower-mass progenitors contributing at later times or metallicity-dependent changes in the yield-weighted IMF, could possibly account for the [α/Fe] break without having to invoke SN Ia's at all. They do not argue that this *is* the explanation of the break, but warn against blindly following the standard framework.

1.3 This work

The variety of astrophysics implicated in the interpretation of the break means it is useful to investigate the range of [α/Fe] ratios found in halo and disc stars around [Fe/H] $\simeq$ -1.0, for example to see whether we are merely comparing two trends in distinct but overlapping populations, halo stars dominating at [Fe/H] < -1.0, and disc stars at [Fe/H] > -1.0. The present paper investigates [Ti/Fe] in high-velocity stars at [Fe/H] > -1.0 identified in the subdwarf analyses of Laird et al. (1988a) and Ryan & Norris (1991a). Since these objects came to our attention by virtue of unusual characteristics, we should not be surprised if a larger than normal fraction of them are affected by sizeable errors. The purposes of this work were first to verify the metallicities and kinematic properties of the stars, second to clarify the stellar population to which they belong, thirdly to measure relative element ratios of an α-element, and finally to consider the implications for the evolution of the Galaxy.

Since their metallicities had been based on photometric colors or very low S/N spectra only, it was necessary to re-measure their metallicities through high-resolution spectroscopy. Iron and titanium were studied, for several reasons. Firstly, in other halo and disc stars, [Ti/Fe] is observed to follow the same abundance trends as other α-elements, even though the reason for this has eluded astronomers for decades. (Recent calculations of nucleosynthesis in SN IIs whose kinetic energy exceeds 10^{51} erg may solve the mystery (Nakamura et al. 2001).) Secondly, titanium has several advantages over other α-elements in a spectroscopic analysis: its lines are numerous in G-dwarf spectra, permitting an average over many lines to improve the accuracy of the measurement, and, more importantly, the atomic structure of Ti is more like that of Fe than are lighter α-elements such as O, Mg and Si. Consequently the effects of some systematic errors in the abundance analyses are minimised by measuring [Ti/Fe]. In order to provide a more reliable comparison of disc and halo star abundances, the same spectral lines, temperature scale, and source of model atmospheres was used for all stars in this study.

In Sect. 2, the selection of the program halo stars is discussed. A number of disc stars were included for comparison purposes. The observations and spectral analysis are discussed in Sect. 3 and 4, followed in Sect. 5 by a discussion of the results.

2 SAMPLE

Stars with high space velocities typical of halo stars but disc-like metallicities, found in the subdwarf analyses of Laird et al. (1988a) and Ryan & Norris (1991a), constituted the primary sample for the investigation.

Errors in proper motions can result in a disc star being misclassified kinematically as a halo object. To minimise these errors, two independent proper motion measurements were sought for each candidate star, using data from the Lowell Proper Motion Survey (Giclas, Burnham & Thomas 1971,1978), Luyten's (1979,1980) NLTT catalog, or the Tycho catalogue (Hog et al. 2000). In a preliminary list of twelve candidate stars which had high velocities and metallicities, updated proper motions supplied by T. E. Corbin (1991, priv.comm.) showed that eight had grossly erroneous proper motions, and were in reality normal disc stars, while for the remaining four stars the proper motions were reasonable (more or less). We return to the issue of proper motions below, but we note here that such a high error rate, 8/12, is not unreasonable for a sample selected on the basis of weirdness, and does not reflect the quality of the input catalogues on the whole.

The ten high-velocity stars observed here are described in the first half of Table 1, while the second half contains data for comparison stars belonging to the disc. Columns (2) and (3) give the coordinates of the stars, with equatorial coordinates in the first record and, for the halo stars, Galactic coordinates l and b to the nearest degree in the second record.

The photometry listed in columns (4)-(5) and the initial [Fe/H] value (column (6)) are from the references in the second record of column (6). Values of [Fe/H] from CLLA (Carney et al. 1994) are based on high-resolution, low-S/N spectra, whereas the remaining halo star metallicities are from photometry. For the disc stars, initial [Fe/H] values are based on previous spectroscopic analyses. Stellar atmospheric parameters and the iron and titanium abundances derived in this work from neutral lines are given in columns (7)-(11); these are discussed in Section 4.

Proper motions (arcsec yr^{-1}), position angles (degrees) and their sources are in columns (12)-(14). All but one object, G172-38, have at least two independent proper motion measurements. For G172-38, Giclas et al. publish 0.48 arcsec/yr, but Luyten does not list it at all, despite his catalog extending down to 0.18 arcsec/yr. Nevertheless, it has a radial velocity of -192 km s^{-1} which, for a star roughly in the direction of the forward solar motion, is suggestive of true high-velocity status. Radial velocities (km s^{-1}) and their sources are given in column (15). Entries with errors quoted (1σ) are from this work, whereas those referenced to CLLA and NR have 1σ uncertainties of $\simeq 1$ km s^{-1} and $\simeq 7$ km s^{-1} respectively.

Distances (pc) are given in column (16). Those with stated errors are from Hipparcos (ESA 1997). For halo stars, distances labelled 'R' were computed by the UBV technique of Sandage (1969; Sandage & Kowal 1988) which assumes main-sequence membership, as implemented by Ryan (1989). In two cases, distances were also available from Hipparcos parallaxes, and in these cases the photometric distances exceed the Hipparcos ones by 27-29%. It is possible, though not certain, that a similar error affects other high-velocity stars. For a third halo star, CD$-53°$3257, a substantially smaller distance was obtained from the VizieR website⋆ under the Hipparcos and Tycho catalogues, though neither catalogue separately seems to list the value. This distance suggests that the star is 3.4 mag fainter than the adopted main sequence; we discuss it again below. For the disc stars, distances were based on Bright Star Catalog (Hoffleit 1982) and Hipparcos Catalogue parallaxes.

Heliocentric space velocities (km s^{-1}), derived where possible from data on the same line of the Table, are listed in columns (17)-(19). U, V and W are positive in the directions (l,b) = (180^o,0^o), (90^o,0^o), and $b = +90^o$.

3 OBSERVATIONS

For five of the high-velocity stars and all of the disc stars, spectral regions approximately 60 Å long centred near 4567 Å and 5010 Å, containing relatively unblended Fe I, Fe II, Ti I and Ti II lines, were observed using the 2.7 m telescope and conventional coudé spectrograph with a TI CCD at McDonald Observatory in October 1991, at a resolving power R = 25000 and S/N$\simeq$80-150 pix^{-1} with ∼4 pixels per resolution element. A spectrum of scattered sunlight was also recorded, and reduced and analysed along with the programme stars. G113-49 and the four stars with declinations south of -20^o were observed with the coudé échelle spectrograph (UCLES) and a Tek CCD at the 3.9 m Anglo-Australian Telescope, at $R = 44000$ and S/N$\simeq$50-100 pix^{-1} with ∼3.5 pixels per resolution element. As the resolution at the 2.7 m telescope was slightly poorer, some spectral lines were blended and could not be utilised.

The lines used in the analysis are presented in Table 2. The first four columns provide the wavelength (Å), excitation energy (eV), $\log_{10}\,gf$ and gf source for the transitions. Measured equivalent widths (mÅ) are given in the body of the table. Equivalent widths could be measured reliably down to 10 mÅ, below which uncertainties in continuum placement became too great. A comparison of equivalent widths measured from the Beckers et al. (1976) solar atlas ('Sun' in Table 2) and measured in the scattered sunlight spectrum ('sky') is shown in Figure 1. The agreement

⋆ http://vizier.u-strasbg.fr/viz-bin/VizieR

Table 1. Photometry, atmospheric parameters, abundances, and kinematics

Name(s)	RA 1950 Dec l	b	V	$B-V$ $E(B-V)$	$[Fe/H]_i$ Refs	T_{eff}	log$g$	ξ	[Fe/H]	[Ti/Fe] s.e.	μ s.e.	PA	Ref	v_{rad}	d	U	V	W
(1)	(2)	(3)	(4)	(5)	(6)	(7)	(8)	(9)	(10)	(11)	(12)	(13)	(14)	(15)	(16)	(17)	(18)	(19)
High-velocity stars																		
LP 697-48	211404	−070200	11.03	0.62	+0.0	5960	4.2[a]	2.0	−0.18	+0.08	0.34	113	L	−101 NR	166 R	189	−147	−158
	44	−35		0.03	RN	5810			0.06	0.12	0.13	69	T	−100.9 ± 0.2		141	−29	4
											0.08−0.18	55-85	T			"±50	"±20	"±50
CD−35° 6431	102438	−352427	9.98	0.52	−0.3	6100	4.2	0.5	−0.36	+0.17	0.26	270	L	112 NR	116 R	113	−136	−39
	273	19		0.02	R89	6090			0.05	0.08	0.18	285	T	100.0 ± 0.3		89	−109	2
G265-26	044549	893530	11.40	0.55	−0.43	6020	4.5	0.5	−0.48	+0.27	0.27	184	G	−36 CLLA	197 R	191	−85	−145
	123	27		0.04	CLLA	6000			0.06	0.08	0.26	150	L	−35.3 ± 0.4		186	−158	−20
G113-49	083235	033824	12.53	0.75	−0.78	5150	4.4	1.0	−0.64	−0.03	0.28	136	G	+71 CLLA	200 R	−146	−213	94
	222	24		0.02	CLLA	5210			0.06	0.09	0.27	139	L	69.8 ± 0.2		−138	−213	79
G172-38	010241	491118	11.08	0.76	−0.63	5150	4.8	1.0	−0.75	+0.09	0.48	153	G	−196 CLLA	124 R	−27	−283	−192
	125	−13		0.03	CLLA	5180			0.06	0.11				−192.3 ± 0.4		−25	−280	−193
G232-18	212851	483848	10.53	0.60	−0.57	5740	4.4	1.0	−0.90	+0.36	0.27	286	G	−261 CLLA	116 R	−88	−253	135
	92	−2		0.05	CLLA	5730			0.06	0.08	0.22	287	L	−259.4 ± 0.2		−72	−253	113
BD+5° 3640	180956	052342	10.42	0.74	−0.4	5220	4.6	1.0	−1.06	+0.30	0.77	223	G	+3 E	76 R	−138	−232	77
=G140-46	33	11		0.02	E,RN	5140			0.06	0.10	0.79	222	L			−141	−236	73
			10.43	0.73	−1.36		4.8 ± .1				0.82	218	H	−0.6 ± 1.1	59 ± 7	−116	−192	42
				0.00	CLLA									−2 CLLA				
LP 859-19	151015	−214724	11.27	0.90	−0.4	4790	4.6	1.0	−1.09	+0.24	0.71	264	L	−56 NR	81 R	187	−186	92
=LHS 3038	341	30		0.03	RN	4730	5.0 ± .2		0.08	0.11	0.73	264	H	−52.6 ± 0.3	64 ± 16	158	−148	71
CD−53° 3257	095600	−541000	9.29	0.49	−0.3	6400	4.0[a]	2.0	+0.2		0.39	303	L	23.2 ± 0.5	118 R	211	−58	−17
=HD298812	279	0		0.03	RN,SN	6490					0.39	301	T		25 T	42	−30	−5
CD−24° 9357	104830	−250511	9.94v	0.26v							0.18	170	L	267v PB	340 RB	−198	−336	−56
=HD94033	271	30			R89						0.17	168	T					
Disc stars																		
sky					+0.00	5770	4.6		+0.02	+0.12								
									0.07	0.12								
HD222368	233723	052118	4.13	0.51	−0.21	6190	3.9	1.5	−0.01	+0.02	0.57	139	B	+5 B	13. B	8	−24	−24
=ι Psc					CdS80	6180	3.89 ± .01		0.05	0.08	0.58	139	H	6.3 ± 0.8	13.8 ± 0.2	8	−26	−27
HD 11007	014549	322616	5.81	0.54	−0.24	5940	4.0	1.3	−0.09	−0.01	0.35	330	B	−27 B	26. B	−27	16	40
					CdS80	6030	3.89 ± .02		0.05	0.07	0.34	331	H	−23.2 ± 0.4	27.3 ± 0.6	−24	19	39
HD165341	180256	023034	4.25	0.78	−0.21	5100	4.2	1.0	−0.18	+0.12	1.12	167	B	−7 B	5.0 B	−7	−19	−18
=70 Oph A					CdS80	5190	4.46 ± .01		0.08	0.16	0.97	173	H	−8.5 ± 1.8	5.09 ± 0.04	−5	−19	−15
HD185144	193228	693434	4.68	0.79	−0.24	5120	4.2	1.0	−0.20	−0.16	1.84	162	B	+27 B	5.6 B	−31	43	−18
=σ Dra					CdS80	5150	4.53 ± .01		0.06	0.07	1.84	161	H	26.9 ± 0.2	5.77 ± 0.01	−31	44	−19
HD 4614	004603	573303	3.45	0.58	−0.33	5840	4.2	1.0	−0.22	+0.01	1.22	115	B	+9 B	5.7 B	29	−9	−15
=η Cas					GS87	5830	4.24 ± .01		0.06	0.08	1.22	117	H	9.5 ± 1.1	5.95 ± 0.02	30	−10	−17
HD 10700	014145	−161200	3.50	0.72	−0.31	5280	4.5	1.2	−0.55	+0.07	1.92	297	B	−16 B	3.5 B	−18	28	13
=τ Cet					CdS80	5260	4.51 ± .01		0.06	0.10	1.92	296	H	−14.0 ± 0.2	3.65 ± 0.01	−18	30	10
HD165908	180508	303313	5.05	0.52	−0.46	5910	3.9	1.0	−0.59	+0.06	0.12	306	B	+1 B	17. B	4	−1	9
=99 Her					CdS80	5930	4.06 ± .01		0.05	0.07	0.15	318	H	3.7 ± 0.2	15.65 ± 0.14	5	3	11

a: assumed gravity
v: indicates a variable quantity
References:
Photometry and initial [Fe/H]: CdS80=Cayrel de Strobel et al. 1980; E=Eggen 1980; GS87=Gratton & Sneden 1987; CLLA=Carney et al. 1994; R89=Ryan 1989; RN=Ryan & Norris 1991a,b; SN=Schuster & Nissen 1989;
Proper motions: B=Hoffleit 1982; G=Giclas et al. 1971,1978; L=Luyten 1979,1980; H=ESA 1997; T=Hög et al. 2000;
Radial Velocities: B=Hoffleit 1982; NR=Norris & Ryan 1989, CLLA=Carney et al. 1994; PB=Przybylski & Bessell 1991; Radial velocities with stated errors (1σ) are from this work.
Distances: B=Hoffleit 1982; H=ESA 1997; R=this work (photometric); T=Hög et al. 2000; RB=Rodríguez & Breger 2001; Distances with stated errors are from Hipparcos.

is very good. As will be seen below, analysis of the scattered sunlight spectrum yields [Fe/H] = +0.02 dex, which is very good, but also gives [Ti/Fe] = +0.12 due to blending of some Ti lines. This is considered indicative of the maximum error introduced by blending. HD 165341 and HD 185144 have comparable equivalent widths to the Sun, but all other stars have weaker lines. Furthermore, the solar scattered light spectrum exhibited a larger FWHM than the program star observations, typically 0.35 Å compared to 0.26 to 0.30 Å, so blending in the sky spectrum represents the worst case, especially since many of the programme stars have lower metallicities.

4 SPECTRAL ANALYSIS

4.1 *Solar analysis*

Abundances were computed in LTE using WIDTH6 (Kurucz & Furenlid 1978) and models provided by R. A. Bell (1981, priv.comm.). We began by analysing our spectral lines in the solar spectrum. The choice of solar model atmosphere can influence derived abundances by $\gtrsim$0.1 dex (e.g. Holweger et al. 1991). Since the programme stars cover a 1000 K range of temperatures and a factor of ten in metallicity, it was regarded as inappropriate to base a solar calculation on an empirical model and then attempt to link that to other stars analysed using a theoretical grid

Table 2. Equivalent widths and atomic parameters

λ	χ	log*gf*[a]	Ref	Sun	Sky	697-48	ιPsc	11007	σDra	70OphA	ηCas	-35:6431	265-26	τCet	99Her	113-49	172-38	232-18	+5:3640	859-19
Fe I																				
4547.85	3.55	−1.01	1	85	86	…	78	81	102	104	75	62	65	81	62	91	81	56	68	73
4551.65	3.94	−2.06	2	28	30	…	18	20	35	35	18	15	12	18	8	18	15	…	…	12
4556.93	3.25	−2.71	2	26	…	…	…	17	37	36	17	11	…	19	8	17	…	…	10	17
4561.42	2.76	−3.08	2	37	41	…	26	27	45	50	25	15	18	28	13	23	19	10	19	16
4566.52	3.30	−2.38	1	44	…	…	…	36	58	…	34	19	…	37	18	36	35	11	19	36
4572.86	3.65	−2.81	2	18	21	…	10	13	27	25	12	8	…	12	5	14	…	…	…	…
4574.23	3.21	−2.50	2	42	47	…	29	28	50	50	27	22	…	32	13	29	28	…	17	27
4574.73	2.28	−2.97	2	60	66	…	52	54	78	72	47	31	28	58	29	52	54	28	42	51
4587.13	3.57	−1.74	1	55	56	…	42	48	69	64	43	28	30	49	26	45	43	21	24	42
4991.86	4.22	−1.91	2	19	16	17	…	…	…	33	…	…	…	10	…	20	13	…	…	…
4994.14	0.91	−3.00	1,3	108	103	104	92	94	…	153	88	75	73	…	…	110	111	76	96	136
5001.87	3.88	+0.01	2	164	151	133	138	147	…	215	140	91	88	141	…	134	136	92	110	143
5002.80	3.40	−1.58	2	83:	94	84	73	70	…	132	73	41	41	86	…	76	86	48	61	77
5014.95	3.94	−0.30	1	141	141	114	115	105	…	194	115	73	87	131	…	122	134	78	106	146
5022.24	3.98	−0.53	2	126:	115	109	94	94	…	187	92	65	73	120	…	108	135	69	77	114
5029.62	3.41	−2.05	2	50	…	52	45	42	…	…	42	26	28	56	…	57	51	17	26	…
5031.92	4.37	−1.67	2	25	27	22	17	22	…	…	20	8	…	22	…	25	21	…	…	…
Fe II																				
4576.34	2.84	−2.92	4,5	65	67	…	80	74	52	48	60	54	48	42	56	36	31	34	21	15
4582.83	2.84	−3.10	6	56	…	…	76	67	47	48	55	46	40	35	47	34	19	28	20	13
Ti I																				
4548.77	0.83	−0.30	7,8	72	74	…	56	65	100	104	58	51	56	85	47	86	99	55	78	113
4555.49	0.85	−0.43	7,8	68	…	…	56	57	91	97	53	44	51	76	38	77	87	49	76	100
4999.51	0.83	+0.31	7,8	108	134	99	95	94	…	194	89	79	79	129	…	129	145	88	127	227
5000.99	2.00	+0.00	8,9,10	45	57	44	…	33	…	…	32	19	22	59	…	51	58	21	46	70
5016.17	0.85	−0.52	7,8	65	…	68	55	…	…	98	57	35	47	84	…	72	85	47	72	105
5022.87	0.83	−0.38	7,8	77	79	74	62	64	…	133	65	51	52	98	…	92	118	57	91	145
5024.85	0.82	−0.55	7,8	71	…	71	59	63	…	104	61	43	46	84	…	78	86	51	68	102
Ti II																				
4568.33	1.22	−2.65	11	34	…	…	33	34	…	…	25	28	16	25	21	26	…	15	10	13
4589.95	1.24	−1.79	11	87	79	…	92	90	72	67	77	84	69	68	78	73	63	62	52	56

a: Offsets of +0.05, −0.15, −0.15, and −0.05 were made to the tabulated Fe I, Fe II, Ti I and Ti II log *gf* values; see text for explanation.
References: (1) O'Brian et al. 1991; (2) Fuhr, Martin & Wiese 1988; (3) Blackwell, Petford & Shallis 1979; (4) Schnabel, Kock & Holweger 1999; (5) Hannaford et al. 1992; (6) Kroll & Koch 1987; (7) Blackwell et al. 1982; (8) Grevesse, Blackwell & Petford 1989; (9) Nitz, Wickliffe & Lawler 1998; (10) Blackwell et al. 1986; (11) Martin, Fuhr & Wiese 1988

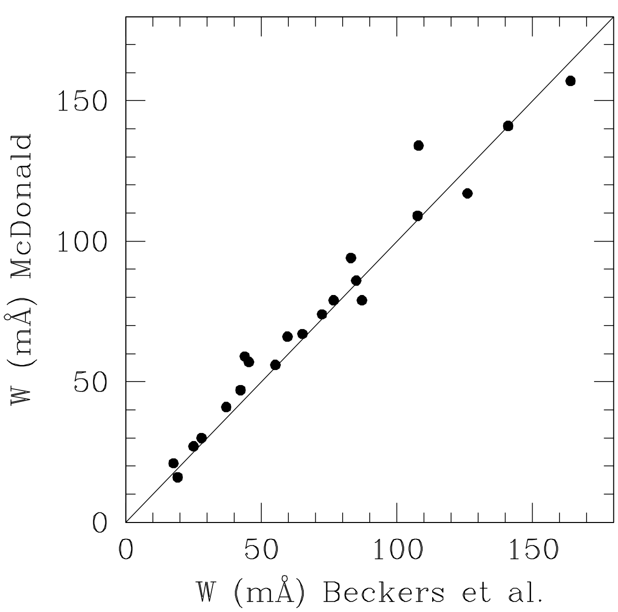

Figure 1. Comparison of equivalent widths measured from the scattered sunlight (sky) spectrum from the McDonald Obs. 2.7 m, and from the Beckers et al. (1976) solar irradiance spectrum.

of models. Instead, the theoretical grid should be used for all calculations. A preliminary computation using the gf values from Table 2 was performed for a Bell model having $\frac{T_{\rm eff}}{\rm K}/\log_{10}\frac{g}{\rm cm\ s^{-2}}/[{\rm Fe/H}]/\frac{\xi}{\rm km\ s^{-1}} = 5770/4.44/0.0/1.0$, and the equivalent widths measured from the Beckers et al. solar atlas (column (5) of Table 2). This yielded abundances $A({\rm Fe})_{\rm I} \equiv \log_{10}\ (n({\rm Fe})/n({\rm H})) = -4.46 \pm 0.04$ from neutral lines and $A({\rm Fe})_{\rm II} = -4.67 \pm 0.02$ from singly-ionised lines, where the subscript indicates which ionisation state was measured. We also obtained $A({\rm Ti})_{\rm I} = -7.15 \pm 0.04$ and $A({\rm Ti})_{\rm II} = -7.02 \pm 0.14$. (Uncertainties are 1 s.e.) These should be compared to the photospheric abundances A(Fe) $= -4.50 \pm 0.05$ and $A({\rm Ti}) = -6.98 \pm 0.06$ (Grevesse & Sauval 1998). A comparison of the Bell model with two empirical models (Holweger & Müller 1974; Fontenla, Avrett & Loeser 1993) showed that the empirical ones, which are almost identical to one another, are up to 250 K hotter than the Bell model through the line-forming regions. For example, the atmospheric level at which $\tau_{5000} = 2/3$ is at 5930 K in the Bell model, but is at 6170 K in the Fontenla et al. model. The lower temperature of the line-forming layers in the Bell model reduces the abundances derived for the Fe I lines, and also reduces the ionisation of Fe, which increases the abundance inferred from Fe II lines relative to Fe I lines. Calculations using the Holweger-Müller model gave $A({\rm Fe})_{\rm I}$

= −4.33, $A(\mathrm{Fe})_{\mathrm{II}}$ = −4.62, $A(\mathrm{Ti})_{\mathrm{I}}$ = −7.00, and $A(\mathrm{Ti})_{\mathrm{II}}$ = −6.94. Because of the higher temperatures, the abundances derived from neutral lines are 0.13-0.15 dex higher, while abundances from the ionised lines are higher by 0.05-0.07.

The intention was to derive surface gravities for the stars from the Fe I-Fe II ionisation balance computed from Bell models, as well as to obtain reliable abundances. Therefore, based on the analysis of the Beckers et al. spectrum, the log gf values for Fe I were increased by 0.05 to reproduce the solar photospheric abundance, those for Fe II were changed by −0.15 to match the derived Fe I abundance and hence imply the correct gravity, and values for Ti I and Ti II were changed by −0.15 and −0.05 respectively. The failure of the initial abundance calculations to match the Grevesse & Sauval values probably reflects systematic differences in the model atmosphere and possibly the neglect of NLTE, rather than poor atomic data. Hence we were reluctant to change the gf's, especially considering the high accuracy attached to many of the laboratory values, but to reproduce the solar gravity and abundance using these lines with Bell models, such a change was necessary.

4.2 *Programme stars*

Since the high-velocity stars have distances up to 200 pc, reddening estimates $E(B-V)$ were made following Laird et al. (1988a) and Ryan (1989), utilising line-of-sight reddening maps. Effective temperatures for all stars were calculated from $B-V$ and in some cases $b-y$ photometry, using the calibrations of Saxner & Hammarbäck (1985) and Magain (1987), which are based on the infrared flux method. The $B-V$ calibration of Buser & Kurucz (1992) was also used, as was their $R-I$ calibration when colors were available. The Buser & Kurucz scale covers a wider range of parameter space, and was required for stars falling outside the Saxner & Hammarbäck and Magain calibrations. Due to the [Fe/H] terms in the color-temperature calibrations, it was necessary to revise the temperature estimates for some stars once a calculation of [Fe/H] based on spectral lines could replace initial estimates. The adopted effective temperatures are presented as the first record in column (7) of Table 1. From the range of effective temperatures given by the calibrations, and photometric uncertainties of order 0.01 mag, the uncertainty in effective temperature is expected to be of order 100 K. As a comparison, the second T_{eff} record for each star gives the value calculated from the $B-V$ calibration of Alonso, Arribas & Martínez-Roger (1996, their Equation 1), to which they assign 1σ errors of 2-3% ($\sim$ 150 K) for stars of this temperature. The mean difference $\langle \Delta T \rangle \equiv \langle T_{\mathrm{RS03}} - T_{\mathrm{AAMR96}} \rangle = 4$ K, with $\sigma_{\Delta T} = 61$ K, which supports the accuracy of the values we have assigned and our adopted error estimate.

Since most of the high-velocity stars are expected to be dwarfs (their high space velocities would be more extreme for subgiants and giants), gravities appropriate to main sequence or turnoff stars were assumed initially, along with microturbulent velocities of 1.0 km s^{-1}. These values were revised in the analysis to eliminate differences in the abundances derived from Fe I and Fe II lines, and to null any dependence of Fe I abundance on equivalent width. The latter yielded values generally in the range 1.0-1.5 km s^{-1}, with two stars giving 0.5 km s^{-1}. Statistical errors in the mean Fe I and Fe II abundances imply a limiting accuracy of $\sigma_{\log g} \simeq 0.15$ by this method. For the disc stars and the two high-velocity stars with Hipparcos distances, surface gravities could be computed and are given in Table 1 in the same line as the Hipparcos distances. These provide a check on the reliability of the spectroscopically-derived gravities, which are on average lower by 0.11 dex, with a standard deviation of 0.19 dex.

The Ti II versus Ti I abundances also provide a check on the gravities. We obtained a reassuringly small mean difference $A(\mathrm{Ti})_{\mathrm{II}} - A(\mathrm{Ti})_{\mathrm{I}}$ = -0.03, with a standard deviation of 0.15.

The decision was taken not to revise T_{eff} using lines of different excitation potential. There were several reasons: The range of Fe I excitation potentials is small; there is only one line at 0.9 eV, which happens to give abundances 0.3 dex lower in the solar analysis for which T_{eff} is known reliably, and above that there are only two lines between 2.2 and 2.8 eV; all the rest are between 3.2 and 4.4 eV. Secondly, the slope that could be fitted to the abundance vs excitation potential data was strongly dependent on whether the suspect 0.9 eV line was retained, and thirdly the derived slope was only marginally significant, $<2\sigma$ when the 0.9 eV line was excluded. The decision was made to retain the 0.9 eV line in the analysis, but not to allow it to dictate T_{eff}.

4.3 *Error propagation*

The [Fe/H] and [Ti/Fe] abundances computed from typically 12-16 Fe I lines and 5-7 Ti I lines are listed in Table 1 (columns (10)-(11)), along with the statistical errors (1σ), and these are plotted in Figure 2. The systematic effects of ±100 K changes in effective temperature are also shown in the Figure, where two lines show the change for stars with effective temperatures of 5100 and 6100 K. A similar inset shows the effects of errors of ±0.25 dex in log g. Errors in microturbulence do not propagate very strongly in [Ti/Fe], as abundances for both elements are affected similarly.

As most of the Fe I lines have high excitation potential, 3-4 eV, they are sensitive to uncertainties in the treatment of damping. The analysis was repeated using damping values for neutral lines from Anstee & O'Mara (1995), Barklem & O'Mara (1997), and Barklem, O'Mara & Ross (1998), and enhancing Unsöld's approximation for the ionised lines by $E_{\gamma} = 0.08\chi_{lo}^2 + 1.30$ (Ryan 1998). Initially the change reduced the Fe I abundances by ~0.1 dex, but after renormalisation of the gf values to reproduce the solar abundance in the analysis of the Beckers et al. spectrum, the change in [Fe/H] was +0.02 dex on average, with star-to-star differences corresponding to $\sigma_{[\mathrm{Fe/H}]} = 0.04$ and $\sigma_{[\mathrm{Ti/Fe}]} = 0.06$. We adopted the usual WIDTH6 analysis as our main results, which uses the damping approximation of Kurucz rather than Unsöld (see Ryan 1998 for details), but included the 0.04 and 0.06 dex errors in the quoted random errors.

4.4 *Two peculiar stars*

Two of the high velocity stars have particularly distinctive characteristics which we set out below.

CD−53°3257 lies more than 0.1 magnitude bluer than the metal-rich main-sequence turnoff in the $U-B$,$B-V$ two-colour diagram, suggesting that it is younger than the halo

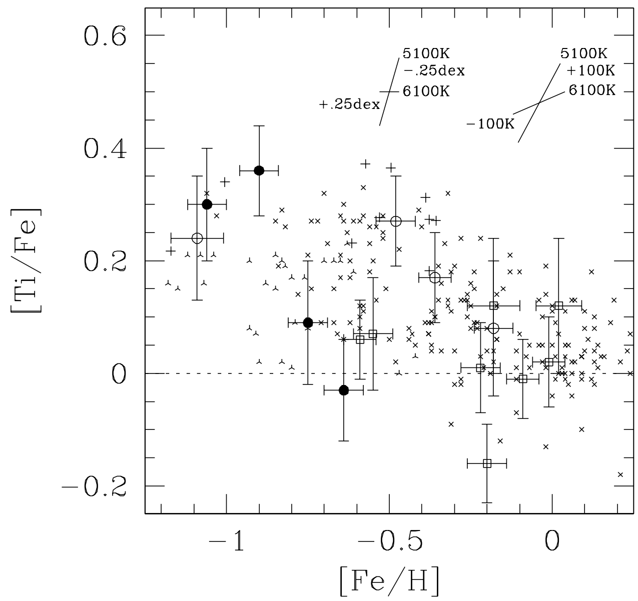

Figure 2. Titanium and iron abundances measured here for possible halo stars (filled circle), probable thick-disc stars (open circle), and thin-disc stars (open squares). Crosses: Edvardsson et al. (1993); plus signs: Prochaska et al. (2000); three-spikes: Nissen & Schuster (1997). Errors bars are 1 s.e. The two large crosses at upper right indicate the systematic effects on stars with T_{eff} = 5100 and 6100 K of revising the adopted temperatures by ±100 K and $\log_{10} g$ by ±0.25 dex.

subdwarfs, or a blue straggler. If the former, the Revised Yale Isochrones (Green, Demarque & King 1987) suggest an age no more than 6 Gyr. Its spectrum shows significant line broadening, which we attribute to stellar rotation. A synthetic spectrum was computed and broadened using an analytic rotation profile from Gray (1992, equation 17-12 with $\epsilon = 0.6$). A speed $v\sin i = 38 \pm 4$ km s^{-1} was found to reproduce the observed line widths, a value which is characteristic of early F dwarfs. Spectra taken 1.1 day apart yielded no evidence for radial velocity variation.

The large rotational velocity prevented a thorough spectral analysis; many of the lines are blended, and their greater breadth increases the error in equivalent width measurements. However, the Mg b triplet provides strong lines which can be analysed. A spectrum synthesis adopting the model parameters in Table 1 gives [Mg/H] = +0.20 ± 0.15, where the uncertainty reflects fitting errors. Changing the assumed log g from 4.0 to 4.5 would decrease this by 0.3 dex. (However, a VizieR search of gives a parallax of 40±15 mas, which implies a low luminosity corresponding to log g = 5.1-5.8!) The metallicity of the star is thus close to solar. Comparison of its spectrum with that of Procyon confirms its metallicity to be roughly solar; unblended lines in CD−53°3257 have slightly greater equivalent widths than those in Procyon (Steffen 1985) but are comparable, consistent with the slightly lower temperature of CD−53°3257. In particular, Ca is not seriously deficient. The low abundance inferred from the Ca II K line by Ryan & Norris (1991a) (viz. -2.39) is not understood, but the superior spectrum obtained in the present work clearly agrees with UBV and Strömgren photometry that its metal abundance is near solar.

CD−24°9357 (HD 94033) was conspicuous because it has a high proper motion but is considerably bluer than the Population II main sequence turnoff, having B-V = 0.26 (but variable; see below). Przybylski & Bessell (1979) identified it as a Pop. II dwarf cepheid, on account of it rapid radial velocity variations of several tens of km s^{-1} over a few tens of minutes, its high space motion associated with a retrograde, highly-elliptical orbit, and its low metallicity (1/30th solar). Its absolute magnitude, M_V = 2.29 (Rodríguez & Breger 2001), implies a distance of 340 pc and a transverse velocity of 282 km s^{-1}, which complements Przybylski & Bessell's radial velocity of 267 km s^{-1}, and supports Rodríguez & Breger's designation of this star as an SX Phe variable. This metal-poor star clearly satisfies our aim of identifying Population II stars of *potentially* uncommon youth; indeed, McNamara & Budge (1985) infer an evolutionary age of 6 Gyr. However, rather than its colour implying youth, the mysterious SX Phe class probably comprises blue stragglers that lie in the instability strip, and hence may owe their properties to post-red giant evolution and/or a stellar merger (Rodríguez & Breger 2001). The existence of SX Phe stars in globular clusters (e.g. Nemec et al. 1995) indicates that their colours certainly do not guarantee youth. No further analysis will be presented here.

5 DISCUSSION

5.1 *[Fe/H] values*

Interest in BD+5°3640 and LP 859-19 had been prompted by their apparently high metallicities, [Fe/H] = -0.4, inferred from UBV photometry. The measurement of much lower abundances, [Fe/H] ≃ −1.0, from high resolution spectra, was not totally surprising. This identifies these two objects as conventional high-velocity stars whose previous metallicity estimates lay at the extreme end of the error distribution. As discussed in connection with proper motion measurements, we should not be too surprised to flush out a higher than normal fraction of erroneous measurements when observing a sample chosen for the weirdness of its members. Two other stars whose preliminary metallicity came from UBV photometry, CD−35°6431 and LP 697-48, were confirmed as having high abundances.

The five stars from the Carney et al. (1994, CLLA) study had previous [Fe/H] values determined by comparing high resolution, low S/N spectra, with a grid of synthetic spectra. In all cases similar metallicities have been derived in the current work, the new values being higher on average by only 0.01 dex, with $\sigma_{\Delta[\mathrm{Fe/H}]} = 0.24$. The mean difference between the abundances derived here and previous spectroscopic analyses for the seven disc stars (excluding the Sun) was similar, Δ[Fe/H] = 0.02 dex and $\sigma_{\Delta[\mathrm{Fe/H}]} = 0.16$ dex.

5.2 *Kinematic assignments*

For CD−35°6431 and LP 697-48, the high proper motions given by Luyten are not substantiated by Tycho measurements, thus reducing the speeds of these stars. Nevertheless, both have large radial velocities (+100 and −101 km s^{-1}) which ensure that high V- and U-velocities respectively survive.

By adopting Gaussian velocity dispersions $\sigma_{U'}$, $\sigma_{V'}$, and

$\sigma_{W'}$, rotational lag velocities $V'_{\rm lag}$, and normalisations for the thin disc, thick disc and halo, it is possible to calculate the relative probabilities that a star from each Galactic component would possess a given (e.g. observed) set of space velocities, and hence to infer to which population each star is most likely to belong, based on these parameters. (The primes indicate velocities relative to the LSR.) Additional criteria could be used, such as the metallicities of the stars if the metallicity distributions are known reliably, but as we presume *not* to know the halo metallicity distribution at [Fe/H] $\gtrsim -1$, we proceed using only the velocity distributions and normalisations. We perform a comparison using the kinematics parameters and normalisations adopted by Norris & Ryan (1991). Specifically, we adopt for the thin disc, thick disc and halo respectively: $\sigma_{U'} = 30$, 74-102, and 145 km s^{-1}, $\sigma_{V'} = 21$, 52-71, and 95 km s^{-1}, $\sigma_{W'} = 16$, 40-55, and 95 km s^{-1}, and $\langle V'_{\rm lag}\rangle = 5$, 31-64, and 190 km s^{-1}. We adopt the relative normalisations 1:0.06-0.02:0.00125. The range of values given for the thick disc reflects greater uncertainty in the parameters of that population. (Wyse & Gilmore (1995) use $\sigma_{W'} = 19$ and 42 km s^{-1} for the thin and thick discs.)

It is far from certain that Gaussian velocity dispersions and a single lag velocity constitute a reliable description of the stellar content of the thin disc, containing as it does stars having a range of ages and scale heights. However, since we are concentrating only on a restricted range of spectral classes corresponding to 5000-6000 K, and should encounter only the kinematically hotter stars amongst our kinematically-selected targets, it probably constitutes an adequate approximation for the purpose at hand. As it turned out, only one of the high-velocity stars in the sample was found to be possibly associated with the thin disc.

We also note that we make no distinction between possible subcomponents of the halo, such as a non-rotating, accreted, high-halo component and a rotating, contracted, low-halo component (Norris 1994, Carney et al. 1996, Carney 2000). In practice, it could be difficult to distinguish the latter component, i.e. a prograde, flattened halo component from thick-disc stars in the lagging tail of the thick-disc V' distribution.

We find that CD$-24°$9357 and LP 697-48 are the only certain halo members. G232-18, G113-49 and BD$+5°$3640 have roughly equal probability (within a factor of two) of being halo or thick-disc members, depending on the uncertain thick-disc parameters. All of the other high-velocity stars are almost certainly thick-disc objects (with the possible exception of CD$-53°$3257 which would be a thin-disc object if the smaller of the two distances in Table 1 were correct). Wyse & Gilmore (1995) suggested that the kinematically cold thin disc has a substantial tail to metallicities below [Fe/H] = -0.4, the metallicity range in which most of our stars lie. Our finding that most of our stars are thick-disc, rather than thin-disc, objects does not contradict Wyse & Gilmore's conclusions, since our selection criteria have favoured kinematically hot stars and hence excluded thin-disc objects.

It is perhaps surprising that even stars with sizeable $V_{\rm lag}$ velocities should be more likely to be thick-disc rather than halo members. This comes about because of the far greater fraction of stars belonging to the thick disc than the halo, by a factor of 10-60 depending on the normalisation. For example, if the thick-disc parameters are $\langle V'_{\rm lag}\rangle = 31$ km s^{-1} and $\sigma_{V'} = 52$ km s^{-1} and it accounts for 0.06 of the solar neighbourhood, while halo stars have $\langle V'_{\rm lag}\rangle = 190$ km s^{-1} and $\sigma_{V'} = 95$ km s^{-1} and make up only 0.00125 of the solar neighbourhood, then amongst stars with $V'_{\rm lag} = 190$ km s^{-1} (and U' and $W' = 0$), the thick disc will still out-number halo stars 3.5:1! This conclusion can be avoided only by revising the halo/disc normalisations, changing the velocity parameters of the populations, or truncating the assumed Gaussian velocity distributions well within 3 standard deviations.

We conclude with a note a selection effects. The stars in this work were adopted from the kinematically-biased studies of Laird et al. (1988a) and Ryan & Norris (1991), which selected stars with high proper motions and hence high transverse velocities. Such samples carry many kinematic biases (e.g. Ryan & Norris 1993), but this fact will not affect the accuracy of the population assignments made above. The reason is straightforward: a star moving with specified velocity components (U,V,W) will have the same radial and transverse velocities, and hence be subject to the same kinematic selection effects, irrespective of any population label we put on it. The survival probability of a star *with a given space velocity* is therefore proportional to the parent fractions rather than the details of the kinematic selection processes. This is what we have assessed above. On the other hand, we could not so easily derive the parent distributions of the contributing stellar populations as functions of velocity, without also going through some model-dependent analysis that accounts for the different survival fractions of stars having different velocities, using, for example, Monte-Carlo techniques (e.g. Norris & Ryan 1991, Ryan & Norris 1991a, 1993).

5.3 *[Ti/Fe] values*

Previous observations of disc stars exhibit a decrease in [Ti/Fe] from ∼0.3 to 0.0-0.1 as [Fe/H] increases from -1.0 to about 0.0 (Edvardsson et al. 1993). The abundances derived here are broadly consistent with such a behaviour (see Figure 2).

The definite halo star (ignoring the SX Phe star) has [Fe/H] = $-0.75 \pm 0.06(1\sigma)$ and [Ti/Fe] = $+0.09 \pm 0.11(1\sigma)$. This measurement suggests a decreasing [Ti/Fe] ratio in the more metal-rich halo stars, though given the large uncertainty in [Ti/Fe] a value typical of more metal-poor halo stars, [Ti/Fe] $\simeq 0.3$, could not be ruled out. If we also consider the three stars which could be either halo or thick-disc members, stronger evidence is found for decreasing [Ti/Fe] with increasing [Fe/H], as the most iron-rich of these, G113-49, has [Fe/H] = -0.64 ± 0.06 and [Ti/Fe] = -0.03 ± 0.09.

Amongst the probable thick-disc stars, LP 697-48 has a high [Fe/H] = -0.18 ± 0.06 coupled with [Ti/Fe] = $+0.08 \pm 0.12$, though we caution that no ionised lines were measured for this star so its gravity is assumed. This and the other thick-disc objects suggest that [Ti/Fe] decreases with increasing [Fe/H].

The range of [Ti/Fe] values is consistent with that found by Nissen & Schuster (1997) for their halo sample, but the decreasing trend with [Fe/H] found here is an interesting contrast to the thick-disc sample of Prochaska et al. (2000) who found consistently high [Ti/Fe] values in their objects. Although we have labelled most of our high velocity stars as probable thick-disc objects, there is a kinematic distinction between our thick-disc stars and Prochaska's: the stars chosen by Prochaska et al. have only moderate $V'_{\rm lag}$ velocities, the largest being 85 km s^{-1}, whereas the thick-disc objects in our sample have much greater values, generally exceeding 100 km s^{-1}. That is, our high-velocity sample contains kinematically extreme thick-disc stars that were initially expected to be halo objects (and may yet turn out to be such if the thick-disc kinematic parameters have been overestimated, as could be the case if a rotating, low-halo component has caused the thick-disc parameters to be overestimated).

It is ironic that Prochaska's rapidly-rotating thick-disc sample has halo-like [Ti/Fe] values whereas our slowly-rotating stars have disc-like [Ti/Fe] values! Prochaska et al. make the possible connection, however, between their stars and the bulge, where McWilliam & Rich (1994) have found [Ti/Fe] to be halo-like. It is possible that Prochaska's thick-disc stars, with small $V'_{\rm lag}$, are probing a different population to our ones which we have also labelled as thick disc but which have velocities more comparable to those of halo objects.

Of the stars labelled by Schuster & Nissen as belonging to the halo, HD 103723 and HD 105004 are more likely to be thick-disc stars according to the kinematic criteria employed here, and several other stars have equal probability of being thick-disc or halo objects. Both HD 103723 and HD 105004 fall into Nissen & Schuster's low-[α/Fe] group, which indicates that the association of low-[α/Fe] with extreme kinematics may be further weakened, since they are less extreme than some of the halo stars. Clearly, further investigation of these issues is warranted.

5.4 *Implications of [Ti/Fe] values for Galactic Chemical Evolution*

As discussed in the introduction, changes in [Ti/Fe] and possibly kinematics at [Fe/H] $\simeq -1$ are often used as constraints in Galactic chemical evolution models (e.g. Wyse & Gilmore 1988, Smecker-Hane & Wyse 1992). However, we cautioned that these features could be due to a number of other factors: a superposition of Galactic components rather than an evolutionary sequence, an over-simplified view of the morphology of the break, and the possible importance of alternative frameworks to SN Ia timescales. We now assess how the current observations might be viewed in each of these frameworks.

5.4.1 A superposition of components

If the break merely reflected the superposition of the halo population at [Fe/H] < -1 and the disc population at [Fe/H] > -1, then genuine halo stars at [Fe/H] > -1 should exhibit high [Ti/Fe] ratios. This appears not to be the case, since G172-38 at [Fe/H] $= -0.75\pm0.06$ has low [Ti/Fe] $= +0.09\pm 0.11$, and G113-49, a possible halo star, has [Ti/Fe] $= -0.03$. Consequently, the data support the conclusions of Nissen & Schuster (1997) that metal-rich halo stars do not have uniquely high [α/Fe] values, and hence the overall decline in [Ti/Fe] seen at [Fe/H] > -1 cannot be due *solely* to samples at [Fe/H] > -1 being dominated by disc stars.

5.4.2 The morphology of the break

Although the break in [α/Fe] has often been regarded as well defined in [Fe/H], and used as a constraint in Galactic chemical evolution models, the data for high-velocity stars at [Fe/H] > -1 do not support this. Some metal-rich halo stars appear to follow a similar trend to disc stars. Objects in both this study and Nissen & Schuster's show a range of [Ti/Fe] values at fixed [Fe/H]. This range is not merely due to the presence of overlapping Galactic components, since thick-disc stars having both high and low [Ti/Fe] values can be found, as can examples of low-[α/Fe] halo stars.

Even if SN Ia timescales were responsible for the break, given the range of onset times for SN Ia discussed by Smecker-Hane & Wyse and Kobayashi et al., it would perhaps be surprising to find a well defined break. Likewise, objections to CO-He white dwarf mergers as the source of SN Ia, on the grounds that the break in [O/Fe] may not occur at the required value of [Fe/H], may not stand (though other objections may remain). Similarly, adopting one particular time for the appearance of SN Ia in some Galactic chemical evolution computations, rather than including a distribution of appearance times, may be responsible for some of the difficulties encountered in reproducing observed abundances.

5.4.3 Alternative frameworks

Kinematic and chemical evidence suggests that many of the high-velocity halo stars with [Fe/H] < -1.0 did not participate in a dissipative collapse such as that which formed the Galactic disc (Norris & Ryan 1989, 1991; Carney et al. 1990a; Ryan and Norris 1991a). Whether *some* metal-poor stars participated in such a collapse depends on the accuracy of proposals that the halo contains more than one component (e.g. Norris 1994, Carney et al. 1996). However, it is difficult to reconcile merger explanations for the origin of metal-rich, high-velocity stars if they obey the disc [α/Fe] trend, as the ones here seem to, since the star-formation history both in fragments and in the disc are unlikely to lead to changes in [Ti/Fe] at the same values of [Fe/H].

Does this suggests that the metal-rich halo stars must have originated within the Milky Way? Not necessarily. If the majority of our high-velocity stars were halo members, then their tendency to follow the disc [Ti/Fe] vs [Fe/H] pattern would make it necessary to conclude that either the metal-rich high-velocity stars did not originate in independently-evolving fragments, or else some mechanism other than star-formation history coordinates the chemical enrichment histories. (If the majority of our stars are in reality thick-disc objects formed in a dissipative collapse then this conclusion is avoided. It would also be avoided if just a few metal-rich halo stars have low [α/Fe], but the Nissen & Schuster study and this one suggest the fraction is not low.) Two possible mechanisms for coordinating chemical enrichment that are not tied so closely to the star-formation history are those proposed by Kobayashi et al. (1999) and Chieffi et al. (2000). In these, the physics of mass accretion in single-degenerate SN Ia progenitors and/or the mass dependence of SN II yields are more important than timing in determining the chemical evolution of the break.

Kobayashi et al. suggest that the single-degenerate origin of SN Ia is active only at [Fe/H] > -1. If this is correct, then the existence of stars with low [α/Fe] at [Fe/H] < -1 might require the double-degenerate mechanism to be the sole SN Ia source at low metallicity. That is, the break might coincide not with the first appearance of SN Ia, but rather the first activation of the single-degenerate pathway, being one of two SN Ia mechanisms. The double-degenerate pathway would be responsible for the rare instances of low [α/Fe] at lower metallicity.

5.5 *Implications for the halo metallicity distribution*

The low-metallicity portion (90%) of the halo metallicity distribution, measured by Laird et al. (1988b) and Ryan & Norris (1991b), is extremely well fit by the modified simple model (Hartwick 1976), but there is an excess of higher metallicity stars.† The analysis in the present paper allows the following comments to be made.

The downward revision of [Fe/H] values for three of the stars in Table 1 by more than 0.3 dex reemphasises that measurements lying in the wings of the metallicity distribution are more likely to have been affected by errors, since stars with [Fe/H] $\simeq$ -1.0 which are subject to negative metallicity errors will merge with the bulk of halo stars and the errors may not be noticeable, whereas those with positive errors will stand out as abnormally metal-rich. This makes it more important that abundances in the wings be verified through high-S/N, high-resolution analyses. Ryan & Norris (1991b) conducted high-S/N, high-resolution analyses of stars in the low-metallicity tail of the distribution, so the low-metallicity end should be accurate, but it is possible that the metallicity distributions are over-populated at the high-metallicity end.

The rejection of several older proper motion measurements (Section 2) and the analysis of kinematics (Section 5.2) emphasises that objects in a proper-motion-selected sample may have substantial contamination by thick-disc objects, particularly at higher metallicity where the number of contaminating objects is larger. The proper-motion-selected samples assembled by Laird et al. and Ryan & Norris reduced thick-disc contamination by admitting only those stars with the most extreme space velocities, but even so some contamination by thick-disc stars may have occurred at the highest metallicities if the population assignments made in Section 5.2 are correct.

The effect of population contamination of the metallicity distribution could be reassessed as follows. A population-weighting factor $P_{\rm h}(U',V',W')$ could be introduced for each star to scale its contribution to the total distribution, where $P_{\rm h}(U',V',W')$ is the probability that a star with velocities (U',V',W') in the solar neighbourhood is a halo object. (Similar schemes using orbital parameters could be developed for samples extending beyond the solar neighbourhood.) The weighting factor, and hence the resulting metallicity distribution, would clearly be model-dependent, but so too are the current ones which implicitly assume there is no contamination, i.e. that all $P_{\rm h}$s are unity. A correction factor such as this will be applied in a forthcoming reanalysis of the halo metallicity distribution.

A complication to efforts to determine the halo metallicity distribution arises once a multiple-component halo (Norris 1994, Carney et al. 1996, Carney 2000) is contemplated. Then one must re-address how to define the component being sought, and how well a rotating, contracted, low-halo component could be distinguished from the thick disc. The assignment of probabilities to each contributing object in the metallicity distribution may be the only tractable way of allowing for population overlaps, since some stars cannot be assigned with certainty to just one Population.

† It is perhaps surprising that such a simple model does so well at reproducing the observations, but it does. That in itself indicates that the chemical enrichment of the halo was dominated by a few simple principles in spite of the existence of separately-evolving fragments.

5.6 *U velocities*

The chemical composition of CD$-53°$3257 is close to solar, and it appears no older than 6 Gyr. Table 1 sets out two distance estimates, one assuming main-sequence membership and the second using a value from the VizieR database. The second value implies a luminosity below the main-sequence and a surface gravity log $g = 5.5$. The greater distance implies kinematics typical of thick-disc membership, whereas the lesser distance implies it is a thin-disc object. If the former distance is correct, CD$-53°$3257 is a candidate for being a late-type counterpart to the Rodgers et al. A-stars which share the properties of youth, approximately solar metallicities, and kinematics more extreme than the disc but with a vertical velocity dispersion lower than that for Population II subdwarfs.

Although there is no age estimate for LP 697-48, these two stars have three similarities: near-solar compositions, kinematics dominated by U velocities, and being confined to the Galactic plane. LP 697-48 could be another counterpart of the A-stars identified by Rodgers et al. (1981). Alternatively, it is possible that both are otherwise-normal disc stars which have been accelerated by some dynamical interaction with a binary.

The large U velocities mean these stars spend part of their time in the inner parts of the Galaxy. It is interesting to note that the metal-poor disc sample identified by Beers et al. (2002) is also characterised by an uncommonly large U velocity dispersion. Their objects with $-1.6 <$ [Fe/H] < -0.6 have $\sigma_U = 122 \pm 26$ km s^{-1}, whereas comparison objects in this metallicity range gave $\sigma_U = 69 \pm 3$ km s^{-1}. Large U velocities may be a characteristic of a poorly understood population of stars spanning a wide range of metallicity and confined to the Galactic plane.

It is interesting to speculate whether these two stars are related to ones that Raboud et al. (1998) and Grenon (2000) have highlighted on account of their anomalous U velocities.‡ The latter are stars currently in the solar neighbourhood, lagging the Sun's rotation by $>$30 km s^{-1}, and possessing U velocities that are systematically positive. That is, there are more stars in the solar neighbourhood with increasing galactocentric distance than there are stars moving towards the Galactic centre. Raboud et al. and Grenon

‡ The authors are grateful to Prof. B. W. Carney for drawing their attention to the work by Grenon and colleagues.

have suggested that they originated in the inner part of the Galaxy, and their motion has been influenced by the Milky Way's central bar, whose non-axisymmetric form produces streaming motions which, in the direction of the Sun, are seen as a net outflow of stars. Such stars are characterised by low W velocities and, because of their origin in the inner Galaxy, high metallicities, both of which are characteristics shared by LP 697-48 and CD $-53°3257$, the two most metal-rich stars of our high-velocity sample. The U velocities we have recorded for these two stars are slightly more extreme than those discussed by Raboud et al. and Grenon, but this may merely reflect the kinematic selection criteria we have used. If larger numbers of metal-rich, high-U-velocity stars are found, it will be interesting to compare their characteristics to those of the less extreme stars purportedly scattered by the bar. If they are more correctly associated with the centre of the Galaxy rather than with either the halo or thick disc, then efforts to disentangle the stellar populations in the solar neighbourhood may have to consider yet another kinematically hot Galactic component.

6 CONCLUSIONS

Laird et al. (1988a) and Ryan & Norris (1991a) identified several stars which appeared to have halo kinematics but metallicities more appropriate to the disc. Improved, independent proper-motion measurements have confirmed at least some of these cases. High S/N spectra were obtained of ten high-velocity stars and seven disc stars at $R \geq 25000$, to measure radial velocities and iron and titanium abundances. Some of the previous metallicity estimates of the high-velocity stars were found to be too high, but two were found to have almost solar composition, CD$-53°3257$ and LP 697-48. Both have small W velocities but large U velocities, unlike those of normal disc stars, and might be later-type counterparts to the Rodgers et al. (1981) A-stars, be related to the metal-poor disc stars of Beers et al. (2002), or be stars originating in the central region of the Galaxy which occupy a streaming flow stirred up by the Galactic bar (Grenon 2000). The first of these stars appears to be younger than 6 Gyr. Another star bluer than the Pop. II main sequence turnoff is the SX Phe pulsator, CD$-24°9357$, though its colour probably does not indicate youth since SX Phe stars are seen in globular clusters and are presumably a subgroup of blue stragglers.

Kinematic models of the halo, thick-disc and thin-disc components were used to assign component-membership probabilities to each star. The majority of the high-velocity sample are more likely to be thick-disc rather than halo objects. The most metal-rich "certain" halo object in the sample has $[Fe/H] = -0.75 \pm 0.06(1\sigma)$. It provides more evidence that halo objects exist with metallicities up to [Fe/H] ~ -0.5 dex, following Saha's (1985) identification of distant RR Lyrae stars with the same metallicity, and Da Costa & Armandroff's (1995) measurement of [Fe/H] ~ -0.4 for the globular cluster Terzan 7, which is associated with the merging Sagittarius dwarf galaxy.

The revised metallicities and the new population assignments suggest that previous measurements of the halo metallicity distribution may have overestimated the number of stars in the metal-rich tail. A reassessment of the probabilities of halo membership is likely to reduce this tail and produce an even better match with the modified simple model for Galactic chemical evolution.

The [Ti/Fe] ratios of the high-velocity stars are broadly similar to those of disc stars at the same [Fe/H]. Both halo and thick-disc components exhibit a range of [Ti/Fe] values; the high-velocity (low-rotation) thick-disc stars differ in this respect from the lower-velocity (higher-rotation) thick-disc sample of Prochaska et al. (2000), all of which have high, halo-like [Ti/Fe].

Chemical evolution models which interpret the "break" in [α/Fe] in terms of the timescale for the occurrence of SN Ia encounter the problem that the break is not well defined, and that the evolutionary sequence across the break cannot be clearly delineated. The use of a single time for the appearance of SN Ia in some Galactic chemical evolution calculations may be responsible for the difficulty experienced in matching the observations.

Disc-like [Ti/Fe] abundances for a larger fraction of metal-rich halo stars are difficult to reconcile with the accretion of independently-evolving halo fragments unless other physics coordinates their enrichment patterns. Two possible coordinating mechanisms are the metallicity-dependence of the single-degenerate pathway to SN Ia's (Kobayashi et al. 1999) and/or the mass-dependence of SN II yields (Chieffi et al. 2000). If the former mechanism is correct, then the rare low [α/Fe] ratios at [Fe/H] < -1 may be due to double-degenerate SN Ia's.

ACKNOWLEDGMENTS

It is a pleasure to acknowledge valuable discussions with T. Corbin and J. Norris, to thank J. Tomkin, J. Spyromilio, J. Norris and G. Da Costa for assistance with the spectroscopy, and to thank the referee, Prof. B. Carney, for his suggestions which have improved the manuscript. This work was supported financially by PPARC (PPA/O/S/1998/00658) and the Nuffield Foundation (NUF-URB02).

REFERENCES

Alonso, A., Arribas, S., & Martinez-Roger, C. 1996, A&A, 313, 873

Anstee, S. D. & O'Mara, B. J. 1995, MNRAS, 276, 859

Barklem, P. S. & O'Mara, B. J. 1997, MNRAS, 290, 102

Barklem, P. S., O'Mara, B. J., & Ross, J. E. 1998, MNRAS, 296, 1057

Beckers, J. M., Bridges, C. A., & Gilliam, L. B. 1976, A High Resolution Spectral Atlas of the Solar Irradiance From 380 to 700 Nanometers (USAF)

Beers, T. C., Drilling, J. S., Rossi, S., Chiba, M., Rhee, J., Führmeister, B., Norris, J. E., & von Hippel, T. 2002, AJ, 124, in press

Blackwell, D. E., Booth, A. J., Menon, S. L. R., & Petford, A. D. 1986, MNRAS, 220, 289

Blackwell, D. E., Menon, S. L. R., Petford, A. D., & Shallis, M. J. 1982, MNRAS, 201, 611

Blackwell, D. E., Petford, A. D., & Shallis, M. J., 1979, MNRAS, 186, 657

Buser, R., & Kurucz, R. L. 1992, A&A, 264, 557

Carney, B. W. 1996, PASP, 108, 900

Carney, B. W. 1999, The Third Stromlo Symposium: The Galactic Halo, B. K. Gibson, T. S. Axelrod, & M. E. Putman (eds), ASP Conf. Ser. 165, (San Francisco: ASP), 230
Carney, B. W. 2000 The Galactic Halo: from Globular Clusters to Field Stars, (Liège, Université de Liège), 287
Carney, B. W., Aguilar, L., Latham, D. W., & Laird, J. B. 1990a, AJ, 99, 201
Carney, B. W., Laird, J. B., Latham, D. W., & Aguilar, L. A. 1996, AJ, 112, 668
Carney, B. W. & Latham, D. W. 1985, ApJ, 296, 803
Carney, B. W., Latham, D. W., & Laird, J. B. 1990, AJ, 99, 572
Carney, B. W., Latham, D. W., & Laird, J. B. 1994, AJ, 107, 2240
Carney. B. W., Wright, J. S., Sneden, C., Laird, J. B., Aguilar, L. A., & Latham, D. W. 1997, AJ, 114, 363
Cayrel de Strobel, G., Bentolila, Hauck, B., & Curchod, A. 1980, A&AS, 41, 405
Chaboyer, B., Green, E. M., & Liebert, J. 1999, AJ, 117, 1360
Chen, Y. Q., Nissen, P. E., Zhao, G., Zhang, H. W., & Benoni, T. 2000, A&A, 141, 491
Chieffi, A., Limongi, M., Dominguez, I., & Straniero, O. 2002, in R. Fusco-Femiano & F. Matteucci (eds), Chemical enrichment of intracluster and intergalactic medium, ASP Conf.Ser. 253, 231
Da Costa, G. S. & Armandroff, T. E. 1995, AJ, 109, 2533
Dinescu, D. I., Demarque, P., Guenther, D. B., & Pinsonneault, M. H. 1995, AJ, 109, 2090
Edvardsson, B., Andersen, J., Gustafsson, B., Lambert, D. L., Nissen, P. E., & Tomkin, J. 1993, A&A, 275, 101
Eggen, O. J. 1980, ApJS, 43, 457
ESA 1997, The Hipparcos and Tycho Catalogues, ESA SP-1200
Fontenla, J. M., Avrett, E. H., & Loeser, R. 1993, ApJ, 406, 319
Fuhr, J. R., Martin, G. A., & Wiese, W. L. 1988 J.Phys.Chem.Ref.Data, 17, Suppl . 4 Atomic Transition Probabilities Iron through Nickel
Giclas, H. L., Burnham, R. Jr, & Thomas, N. G. 1971, Lowell Proper Motion Survey, Northern Hemisphere (Lowell Obs., Flagstaff)
Giclas, H. L., Burnham, R. Jr, & Thomas, N. G. 1978, Lowell Proper Motion Survey, Southern Hemisphere (Lowell Obs., Flagstaff)
Gilmore, G. & Wyse, R. F. G. 1991, ApJ, 367, L55
Gratton, R. G., & Sneden, C. 1987, A&AS, 68, 193
Gray, D. F. 1992, The Observation and Analysis of Stellar Photospheres, 2nd edition (Cambridge Uni. Press, Cambridge)
Green, E. M., Demarque, P. & King, C. 1987, Revised Yale Isochrones and Luminosity Functions (Yale Uni. Press, New Haven)
Grenon, M. 2000, The Evolution of the Milky Way, F. Matteucci & F. Giovannelli (eds), (Dordrecht: Kluwer), 47
Grevesse, N., Blackwell, D. E., & Petford, A. D. 1989, A&A, 208, 157
Grevesse, N. & Sauval, A. J. 1998, Spc.Sci.Rev., 85, 161
Hannaford, P., Lowe, R. M., Grevesse, N., & Noels, A. 1992, A&A, 259, 301
Hartwick, F. D. A. 1976, ApJ, 209, 418
Helmi, A., White, S. D. M., de Zeeuw, P. T., & Zhao, H.-S. 1999, Nature, 402, 53
Hernandez, X., Gilmore, G., & Valls-Gabaud, D. 2000, MNRAS, 371, 831
Hoffleit, D. 1982, The Bright Star Catalogue, 4th edition (Yale University Obs., New Haven)
Hög, E. et al. 2000, A&A, 355, L27
Holweger, H., Bard, A., Kock, A., & Kock, M. 1991, A&A, 249, 545
Holweger, H. & Müller, E. A. 1974, Sol.Phys., 39, 19
Ibata, R. A., Gilmore, G., & Irwin, M. J. 1995, MNRAS, 277, 781
Kobayashi, C., Tsuijmoto, T., Nomoto, K. Hachisu, I., & Kato, M. 1998, ApJ, 503, L155
King, J. R. 1997, AJ, 113, 2303
Kroll, S., & Kock, M. 1987, A&AS, 67, 225
Kurucz, R. L. & Furenlid, I. 1979, SAO Special Report 387 Sample Spectral Atlas for Sirius
Laird, J. B., Carney, B. W., & Latham, D. W. 1988a, AJ, 95, 1843
Laird, J. B., Rupen, M. P., Carney, B. W. & Latham, D. W. 1988b, AJ, 96, 1908
Lance, C. M. 1988, ApJ, 334, 927
Luyten, W. J. 1979, NLTT Catalogue I,II (Minnesota, Minneapolis)
Luyten, W. J. 1980, NLTT Catalogue III,IV (Minnesota, Minneapolis)
McNamara, D. H., & Budge, K. G. 1985, PASP, 97, 322
Magain, P. 1987, A&A, 181, 323
Martin, G. A., Fuhr, J. R., & Wiese, W. L. 1988 J.Phys.Chem.Ref.Data, 17, Suppl. 3 Atomic Transition Probabilities Scandium through Manganese
Mateo, M. 1998, ARAA, 36, 435
McWilliam, A., & Rich, R. M. 1994, ApJS, 91, 749
Morrison, H .L., Flynn, C., & Freeman, K. C. 1990, AJ, 100, 1191
Nakamura, T., Umeda, H., Iwamoto, K., Nomoto, K., Hashimoto, M., Hix, W. R., & Thielemann, F.-K. 2001, ApJ, 555, 880
Nemec, J., Mateo, M., Burke, M., & Olszewski, E. W. 1995, AJ, 110, 1186
Nissen, P. E., & Schuster, W. J. 1997, A&A, 326, 751
Nitz, D. E., Wickliffe, M. E., & Lawler, J. E. 1998, ApJS, 117, 313
Nomoto, K., Shigeyama, T., & Tsujimoto, T. 1991, in Evolution of Stars: The Photospheric Abundance Connection, edited by G. Michaud and A. Tutukov, p.21
Norris, J. E. 1994, ApJ, 431, 645
Norris, J. E., & Ryan, S. G. 1989, ApJ, 340, 739
Norris, J. E., & Ryan, S. G. 1991, ApJ, 380, 403
O'Brian, T. R., Wickliffe, M. E., Lawler, J. E., Whaling, W., & Brault, J. W. 1991, J.Opt.Soc.Am.B., 8, 1185
Oswalt, T. D., Smith, J. A., Wood, M. A., & Hintzen, P. 1996, Nature, 382, 692
Peterson, R. C. 1981 ApJS, 45, 421
Preston, G. W., Beers, T. C., & Shectman, S. A. 1994, AJ, 108, 538
Preston, G. P. & Sneden, C. 2000, AJ, 120, 1014
Prochaska, J. X., Naumov, S. O., Carney, B. W., McWilliam, A., & Wolfe, A. M. 2000, AJ, 120, 2513
Przybylski, A. & Bessell, M. S. 1979, MNRAS, 189, 377
Raboud, D., Grenon, M., Martinet, L., Fux, R., & Udry, S. 1998, A&A, 335, L61
Rodgers, A. W., Harding, P., & Sadler, E. 1981, ApJ, 244, 912
Rodríguez, E. & Breger, M. 2001, A&A, 366, 178
Ryan, S. G. 1989, AJ, 98, 1693
Ryan, S. G. 1998, A&A, 331, 1051
Ryan, S. G., & Norris, J. E. 1991a, AJ, 101, 1835
Ryan, S. G., & Norris, J. E. 1991b, AJ, 101, 1865
Ryan, S. G. & Norris, J. E. 1993, Galaxy Evolution: The Milky Way Perspective (ASP Conf.Ser. 49), S. R. Majewski (ed), (San Francisco: ASP), 103
Saha, A. 1985, ApJ, 289, 310
Sandage, A. 1969, ApJ, 158, 1115
Sandage, A., & Kowal, C. 1986, AJ, 91, 1140
Saviane, I., Rosenberg, A., & Piotto, G. 1999, The Third Stromlo Symposium: The Galactic Halo, ed. B. K. Gibson, T. S. Axelrod, & M. E. Putman, ASP Conf.Ser. 165, 308
Saxner, M. and Hammarbäck, G. 1985, A&A, 151, 372
Schnabel, R., Kock, M., & Holweger, H. 1999, A&A, 342, 610
Schuster, W. J., and Nissen, P. E. 1989, A&A, 222, 69
Searle, L. & Zinn, R. 1978, ApJ, 225, 357
Smecker-Hane, T. A., & Wyse, R. F. G. 1992, AJ, 103, 1621

Steffen, M 1985, A&AS, 59, 403
Stetson, P. B. 1981a, AJ, 86, 1337
Stetson, P. B. 1981b, AJ, 86, 1882
Tinsley, B. M. 1979, ApJ, 229, 1046
Tutukov, A. V. & Yungelson, L. R. 1994, MNRAS, 268, 871
VandenBerg, D. A. 2000, ApJS, 129, 315
Wheeler, J. C., Sneden, C. & Truran, J.W. Jr 1989, ARAA, 27, 279
Wyse, R. F. G., & Gilmore, G. 1988, AJ, 95, 1404
Wyse, R. F. G. & Gilmore, G. 1995, AJ, 110, 2771